

Walter J Freeman

A field-theoretic approach to understanding scale-free neocortical dynamics

Received: 5 October 2004 / Accepted: 18 March 2005 / Published online: ■
© Springer-Verlag 2005

Abstract A mesoscopic field-theoretic approach is compared with neural network and brain imaging approaches to understanding brain dynamics. Analysis of high spatiotemporal resolution rabbit electroencephalogram (EEG) reveals neural fields in the form of spatial patterns in amplitude (AM) and phase (PM) modulation of gamma and beta carrier waves that serve to classify EEGs from trials with differing conditioned stimuli (CS+/-). Paleocortex exemplified by olfactory EEG has one AM-PM pattern at a time that forms by an input-dependent phase transition. Neocortex shows multiple overlapping AM-PM patterns before and during presentation of CSs. Modeling suggests that neocortex is stabilized in a scale-free state of self-organized criticality, enabling cooperative domains to form virtually instantaneously by phase transitions ranging in size from a few hypercolumns to an entire hemisphere. Self-organized local domains precede formation of global domains that supervene and contribute global modulations to local domains. This mechanism is proposed to explain Gestalt formation in perception.

1 Introduction

1.1 Networks vs. populations

Attempts to model brain function with model neurons and neural networks have not fared well. The limitation of networks stems from its failure to deal with the hierarchical organization of brains: microscopic, mesoscopic and macroscopic. At the microscopic cellular level the key module is the neuron. Network theory suffices to model neural chains in sensorimotor systems to and from cortex in vertebrate brain stem and spinal cord and in ganglionic chains of invertebrate "simpler systems".

Walter J Freeman
Department of Molecular & Cell Biology,
University of California at Berkeley,
Berkeley, CA 94720-3206, USA
E-mail: wfreeman@socrates.berkeley.edu
<http://sulcus.berkeley.edu>

At the macroscopic brain level the key module is the local area of cortex or nucleus in the cerebral hemisphere that is labeled by imaging differential blood flow and other signs of metabolic enhancement. The intervening mesoscopic level of integration of neural activity into cortical areas, where each neuron interacts with many thousands of other neurons in tissue called neuropil, is not well accessed by either sets of methods. Neuropil cannot be reduced to discrete networks of equivalent neurons; its three types – laminar (cortex), nuclear (basal ganglia) and reticular (periventricular gray matter in the brain stem and spinal cord) – have differing architectures and state variables. The aim of this report is to introduce a field theory as an alternative approach that requires differing definitions, premises, rules of evidence and classic experiments to address the distinctive properties of neural populations.

In classical unit experiments a brief stimulus is typically confined to a single sense modality. The resulting unit activity is tracked through relays that process the stimulus information, and a network is constructed to simulate the processing. In classical behavioral experiments the subjects deal not with isolated stimuli but with environmental *situations*, which are signaled by swarms of sensory receptor action potentials that propagate through the spinal cord and brain, where they modify preexisting unit activity. The impacts of sensory-evoked swarms destabilize cortical neuropil, causing it to jump through successive states.

The goal of field theory is to model these states and state transitions as large-scale spatial patterns of neural activity that quickly lead to motor activity governing the engagement of subjects with their situations. The cortical states constitute "wave packets" that resemble frames in a motion picture (Freeman 2003c, 2004a,c). The rules of evidence in field theory require that brain states be defined as spatial patterns formed by phase transitions; that state variables include carrier waveforms and gating frequencies; and that electroencephalogram (EEG) parameters be validated as meaningful by demonstrating correlations among EEG patterns, situations, subjects' actions, human subjects' descriptions of multi-sensory perceptions (Gestalts) and their meanings (Freeman 2003a).

1.2 Action potentials vs. EEG

Dendritic current regulates action potentials. That same current in cortex is the main source of the EEG as it flows across the fixed extracellular impedance of the neuropil. Due to summation of extracellular electric potentials of dendrites that are oriented in palisades in cortical neuropil, the EEG amplitude expresses the local mean field of unit activity in the neighborhoods of interacting pyramidal cells sustaining local field potentials. This feature endows the EEG with its value for estimating the magnitudes of spatiotemporal state variables in neuropil, both at the mesoscopic network level and at the macroscopic level of the hemisphere but not at the microscopic level. In order to search in the EEG for neural correlates in the pulse activity of single neurons, the assumption required is that there is synchronization of the oscillations in dendritic current of the majority of neurons that contribute to the EEG. Their cooperation is established by the excitatory synapses they give to each other, by which they sustain background activity by mutual excitation (Freeman 2000). The steady activity from this positive feedback loop is made oscillatory by the negative feedback from inhibitory interneurons.

Now the positive feedback is not just disynaptic but also serial through three, four and indefinitely more synapses, so that the feedback path resembles a one-dimensional diffusion process, and the return of output from the pulse of each neuron to itself is a gamma distribution of order one half, that is, randomized (Freeman 1975). The inference follows that the EEG manifests time multiplexing of neurons in cortical hypercolumns that share the load of signal transmission by random rotation of the duty cycle, thereby minimizing the disturbances in extracellular media of the metabolites that accrue with each action potential. The EEG is a correlate of the multiplexed, space-averaged signal output of the local neighborhood, which is very different from the time-averaged output of spike trains from single neurons, because the ergodic hypothesis does not hold for activity of cortical neurons in behaving subjects.

The conceptual framework for units in networks includes the assignment of features, objects and motor commands to the pulse trains of neurons. This framework has been extended by Houk (2005) to networks of digital processing modules (DPMs) that are composed of an array of striatal neurons whose output is a vector formed by a set of pulse trains. Each DPM includes multiple loops through the basal ganglia and cerebellum. Input information is provided primarily by one or more areas of cortex and secondarily by dopamine fibers assigning reinforcement; output directed back to the cortex constitutes instructions for the performance of a skilled action. Networks of DPMs provide for sequences of skilled actions.

In contrast, field theory sees cortical signals as continuously distributed in the neuropil in which the cortical components of DPMs are embedded. It addresses the difficult problems of how the action patterns of wave packets are created, and how they coordinate the outputs of DPMs toward

the goals that are constructed by creative cortical dynamics. The spatial domains of wave packets are described by their boundary conditions and the textured patterns of their carrier waves. Each pattern is displayed as a vector with its tip inscribing an itinerant chaotic trajectory (Tsuda 2001) in brain state space. Its sequential spatial patterns vary in sizes and textures that correlate with cognitive situational behaviors (Ohl et al. 2001, 2003; Freeman 2003a, 2005) of the kind documented by Köhler's field theory (1940), Tolman's (1948) cognitive map, and Gibson's (1979) ecological psychology. Every skilled action involves all cortex and basal ganglia in varying degree.

1.3 Paleocortex vs. neocortex

Neural networks generally treat the evolution of cortex inadequately (Herrick 1948). The first laminated neuropil in primordial vertebrates, three-layered archicortex (e.g. hippocampus) and paleocortex (e.g. the olfactory system), formed a unified sheet comprising each cerebral hemisphere. The best "simpler system" for modeling elementary brain dynamics is olfaction, not vision or audition; the best animal models are rats and rabbits, not monkeys or humans. Paleocortex in mammals is supplemented with a far more complex form of neuropil: six-layered neocortex. Despite its enormous size in humans, neocortex retains its anatomical unity and its dynamics for extremely rapid, repetitive phase transitions with formation of spatial patterns. The specialized neural networks embedded in neocortex operate as input/output interfaces for seeing, hearing, touching and intentional action (Houk 2005). Understanding the integration of their roles in perception is a major aim of field theory.

1.4 K-sets

The proposed basis for a field theory is a hierarchy of nonlinear ordinary differential equations, having noninteractive populations (KO) near equilibrium at its base (Freeman 1975; Principe et al. 2001). By synaptic transmission KO sets create interactive populations of excitatory (KIE) or inhibitory (KII) neurons with nonequilibrium point attractors. KI populations of olfactory excitatory or inhibitory neurons comprise the KII set having also a limit cycle attractor used to model olfactory bulb or prepyriform cortex. The KIII set incorporates three KII sets to model chaotic attractors governing the olfactory EEG (Freeman 1987), and to replicate olfactory capacity for classification of incomplete patterns embedded in complex backgrounds with facilitation by noise (Freeman et al. 1997; Kozma and Freeman 2001). The KIV model of the primordial amphibian paleocortex comprising its limbic system is currently under development as an interactive network of three KIII sets being used by autonomous vehicles for navigation (Kozma and Freeman 2003; Kozma et al. 2003). The new goal is to construct a KV set that models the unique neurodynamics of neocortex found only in mammals.

It is important to distinguish the neuropil as an embedding medium for DPMs from the nets with precisely organized connections that define the DPMs within areas of cortex and within the thalamus, basal ganglia and pons (Houk 2005). Anatomical data already make clear that neocortical neuropil should be seen not only as a network of hypercolumns but also as a unified structure comprising an entire cerebral hemisphere. Its global connectivity cannot be modeled as a random graph with uniform probability of connection lengths. Short connections approximating nearest neighbor predominate; the significant proportion of long connections leads to small-world effects (Watts and Strogatz 1998) by which local activity is seeded to distant sites, so that no neuron in the neuropil is more than a few synapses from any other. Several types of network have been proposed to model (Friston 2000; Linkenkaer-Hansen et al. 2001; Stam et al. 2003; Kozma et al. 2005) the long-distance synchronization that is readily observed in scalp EEG (Rodriguez et al. 1999; Tallon-Baudry and Bertrand 1999; Varela et al. 2001). Quantitative anatomical data have for years (Sholl 1956) shown exponential connectivity distributions among cortical neurons; recent data (Braitenberg and Schüz 1991) show fractal and power-law distribution of cortical connectivity of scale-free networks (Wang and Chen 2003). A goal of field theory is to suggest how to use these concepts to model neocortex as a global organ that stabilizes itself by mechanisms that are to be sketched below (Freeman 2004a,b).

2 Spatial patterns: paleocortical (OB) and neocortical EEG

2.1 Paleocortex

Initially the construction of K-sets was guided by fitting sums of linear basis functions to cortical responses to impulse stimuli, so as to measure and simulate the responses (evoked potentials and poststimulus time histograms) of olfactory neurons to electrical stimuli (Freeman 1975). The K-sets were extended to measuring and simulating changes in background EEG and unit activity in the olfactory system that accompanied odor CS that were reinforced (CS+) or not (CS-). After the training (Freeman and Grajski 1987) the olfactory system generated EEG spatial patterns of AM of spatially coherent gamma oscillations (Fig. 1, a, 30–80 Hz) that were accompanied by spatial patterns of phase modulation (PM) (Fig. 2, b). The method used high-density 8 × 8 arrays of implanted electrodes to resolve EEG spatial texture. The demonstration was generalized to the visual, auditory and somatic cortices with multichannel EEGs from trained rabbits (Barrie et al. 1996) and gerbils (Ohl et al. 2001).

These spatial amplitude-modulated patterns differed in several ways from the impulse responses. Their start latencies varied unpredictably, showing that the AM patterns resulted from destabilization and phase transition that resembled spontaneous symmetry breaking. The information in the AM patterns that served to classify them with respect to CSs was

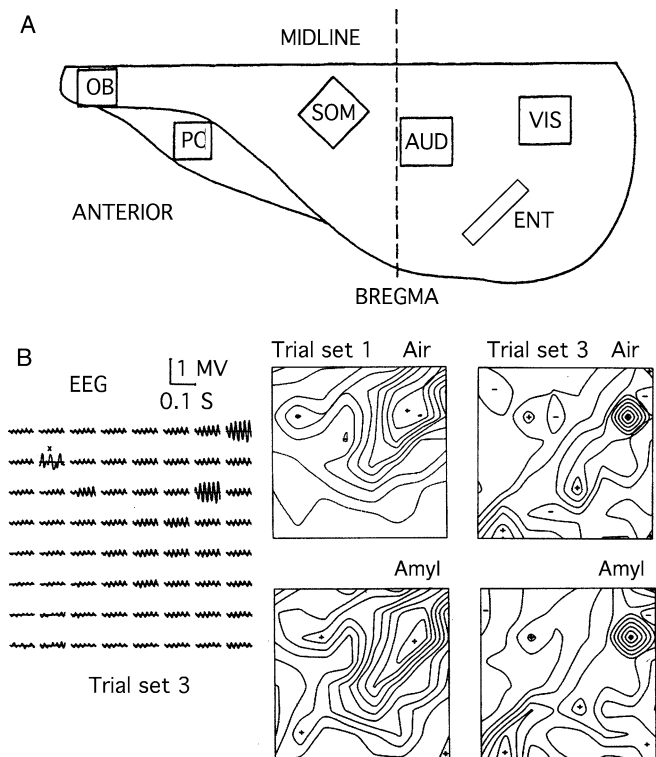


Fig. 1 **a** Squares show the locations on the dorsal surface of intracranial high-density 8 × 8 electrode arrays over the primary sensory areas of the left hemisphere of the rabbit brain. Circles show median and 95% diameter of spatial patterns of phase (half-power phase cone diameters centered on the auditory array). Modified from Barrie et al. (1996). **b** The AM patterns (spatial amplitude modulation of the gamma carrier wave) are shown as contour plots of the root mean square (RMS) EEG. The patterns change with the situation in classical conditioning. From Freeman and Schneider (1982)

homogeneously distributed spatially, not localized, as was the prior sensory information. The AM patterns depended on the context and individual history of each subject.

Electroencephalogram measurement required elementary waves and geometric shapes called “basis functions” (Freeman 1975). Sets of basis functions were adjusted and added like weights on a scale until their sum matched the wave pattern to “decompose” it into its numbered parts. The basis functions tested for temporal patterns came from FFT, PCA, ICA, ARMA, Gabor filters or nonlinear wavelets (Freeman and Viana Di Risico 1986). None of these was fully appropriate for long segments (>256 m) with broad 1/f-type spectra. The most effective basis functions in brief epochs (32–256 m) were root mean square (RMS) for amplitude and a cosine for phase, owing to slow-frequency modulation about the mean within short epochs.

The optimal basis function for spatial patterns of amplitude was the bivariate Gaussian (Freeman and Baird 1987). For spatial patterns of phase in the olfactory bulb, a plane fits the phase gradient of the impulse response (averaged evoked potential) on electrical stimulation of the olfactory nerve, giving a phase velocity equal to the conduction velocity of the afferent axons. The phase gradient of the bursts of gamma

EEG induced by inhalation was not a plane. The conic basis function best minimized by far the least-squares residuals of surface fitting (Freeman and Baird 1987). The location and sign of the apex (phase lead or lag) varied randomly over successive inhalations. Phase cones were minimized or abolished in controls by randomization of channel order, by shuffling (transposition of segments) or by calculating surrogate data (Freeman 2004b). In the olfactory bulb the AM pattern with each inhalation (Fig. 1, b) that classified EEG segments with respect to CS (Fig. 2, a) (Freeman and Grajski 1987) also had phase modulation (PM, Fig. 2, b) – the phase cone – which was interpreted as the residue of a phase transition that was induced by inhalation. Neuropil being a distributed medium, a phase transition spread from a site of nucleation (apex). The conduction velocity of axons parallel to the surface and the frequency of oscillation determined the phase gradient.

2.2 Neocortex

The neocortical EEGs of the visual, auditory and somatic cortices showed that, following classical and operant conditioning of animals to discriminate conditioned stimuli in these modalities, a sequence of two to four AM patterns occurred in the gamma carrier wave. The intermittent AM patterns were classified at better than chance levels ($p < .01$) with respect to the CS on randomly alternating trials (Barrie et al. 1996; Ohl et al. 2001). The hypothesis was confirmed that each AM pattern was formed by an input-dependent phase transition that was manifested in a phase cone (Freeman and Barrie 2000; Freeman 2003b) broad enough to include multiple subareas of sensory cortices (circles Fig. 1, a).

In all areas the classificatory information in the AM patterns was nonlocal; no one electrode was more or less important than any other; the more channels were used, the better was the classification (Freeman and Baird 1987; Barrie et al. 1996; Kozma and Freeman 2002; Ohl et al. 2003). This distributed nature of EEG classificatory information is a characteristic of perception that distinguishes it from the sensory information that is localized by unit recording.

2.3 Hemisphere-wide spatial EEG patterns

Further generalization was achieved by recording EEGs simultaneously from mini-arrays on the left visual, auditory, somatic, olfactory and entorhinal areas of cats and rabbits trained to discriminate CS+/- . The phase and amplitude of the 64 EEG signals were calculated in the species-specific gamma range for each subject (Freeman et al. 2003). Two to three recursive spatial AM patterns were detected between CS and conditioned response (CR) that served to classify EEG segments with respect to CS+ and CS- (Fig. 3, a). The classificatory information was in all recording sites. Removal of data from any of the five areas reduced correct classification, proving that the memory was distributed and dynamic, not

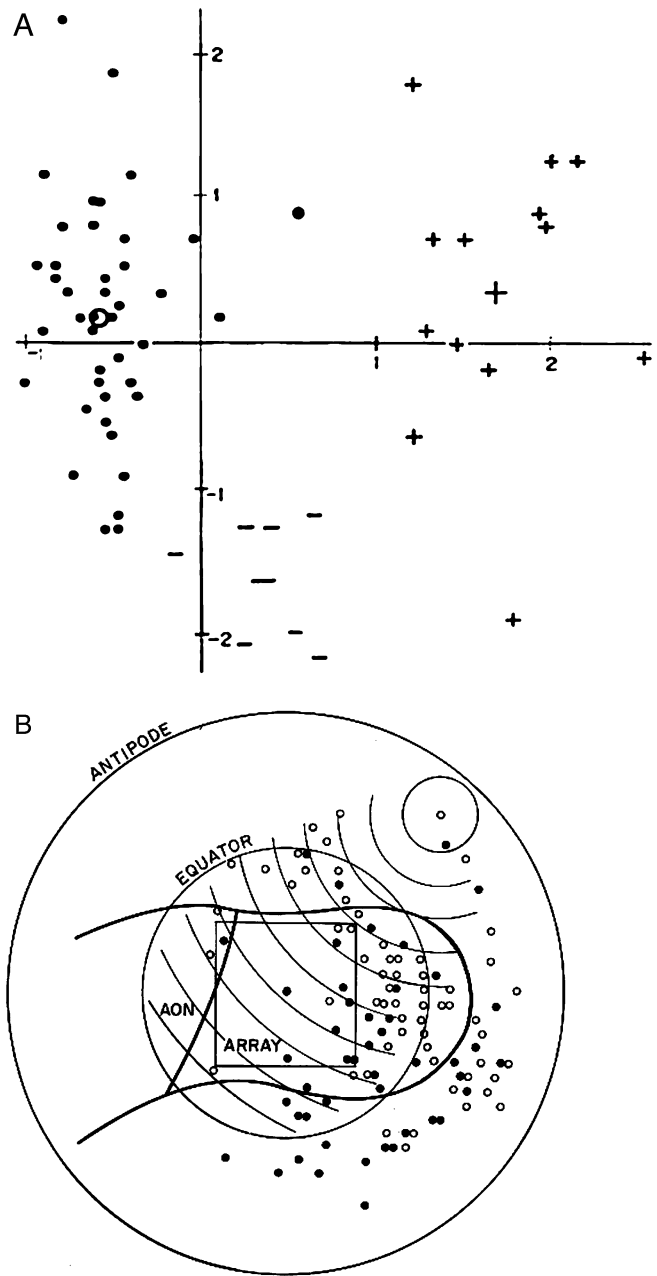


Fig. 2 a Amplitude modulation patterns of EEG gamma bursts had >95% of variance in the first component of PCA. The RMS of each AM pattern gave a point in 64-space. Similar patterns formed clusters, shown here by stepwise discriminant analysis. The clusters show chaotic attractors in brain state space, projected into two-space. From Freeman and Viana Di¼risco (1986). **b** The square shows the outline of the 8 × 8 array [5.6 × 5.6 mm] on the surface of rabbit OB (dark outline). The spherical bulbar surface was flattened to plot the locations of the apices of phase cones from 40 trials. The spatial pattern of phase modulation (PM) conformed to a cone as shown for one burst with isophase contours at intervals of 0.1 rad. The location and sign of the apices varied randomly as shown by filled dots (phase lead) and open dots (phase lag). This PM pattern in OB was found in all neocortical sensory areas (Freeman and Barrie 2000; Freeman 2003b). From Freeman and Baird (1987)

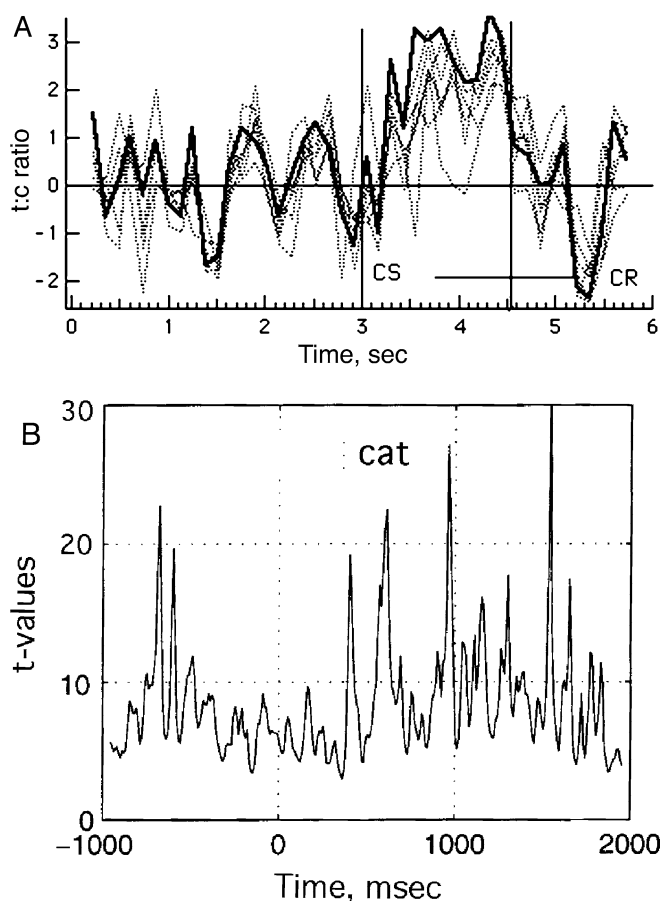


Fig. 3 Neocortical EEG lacked the burst structure of paleocortical EEG that served to locate phase transitions dependent on input. Classification of the RMS AM patterns across 40 trials was done in a moving window 64–128 ms in duration, stepped at 8 ms overlapping intervals. At each step the number of correctly classified patterns among the 40 AM patterns (20 CS+ and 20 CS- randomly interspersed) was calculated. In previous studies of neocortex (Barrie et al. 1996) the 64 electrodes were concentrated on one sensory cortex. Here there were five mini-arrays on the left hemisphere. **a** The *dark curve* shows the level of pattern classification of global EEG segments from randomly interspersed trials in cats with reinforced and unreinforced CS. The *dotted curves* show the decrease in significance level when the data were excluded from the visual, auditory, somatic, olfactory or entorhinal areas, showing that all areas contributed to the classification. From Freeman and Burke (2003). **b** The *curve* shows synchronization among the five areas, measured by the analytic phase. From Freeman and Rogers (2003)

local and static. The largest reduction in goodness of classification resulted from removing the data from the olfactory bulb channels (Freeman and Burke 2003). The analytic phase from the Hilbert Transform (HT) gave a synchronization index (introduced by Tass et al. 1998) that revealed intermittent phase locking of the gamma EEG among all five areas, correlated with maxima in AM pattern classification (Fig. 3, b) (Freeman and Rogers 2002, 2003).

These data led to the hypothesis that the local cortical AM patterns specific to each sensory modality and comprising wave packets were intermingled by being broadcast, and that global spatial patterns formed repeatedly by phase tran-

sitions over large area of each cerebral hemisphere served to integrate the wave packets from the several primary sensory areas into the formation of multisensory Gestalts, as suggested by Fig. 3.

3 Human intracranial and scalp EEG from high-density arrays

3.1 Spatial PSDx for Nyquist frequencies

The basic requirement for spatial pattern analysis is spatial spectral analysis by over-sampling the EEG with a linear array to calculate the spatial power spectral density (PSDx). The concave-upward inflection (Fig. 4, a) defines the upper frequency limit at which noise predominates. That spatial frequency determines the Nyquist frequency, and the spatial electrode interval is half that spatial wavelength. Then an electrode array with that interval will not miss spatial texture nor will the spectra suffer aliasing. This work was done 30 years ago to study EEG patterns in animals. Four years ago for intracranial studies in humans a 1×64 linear array was designed with spacing of 0.5 mm and length 32 mm, short enough to fit onto a single gyrus in neurosurgical patients during exploration to treat epilepsy (Freeman 2000). The PSDx (Fig. 4, a, right curve) indicated an optimal sample interval of 1.25 mm, an order of magnitude closer than the standard clinical array interval of 1 cm to search for textural patterns in subdural EEG. The PSDx showed the $1/f^\alpha$ in log-log coordinates with $\alpha \sim 2 \pm 1$ already found in rabbits (Freeman 2004a).

A linear 1×64 array was designed for scalp EEG with spacing of 3 mm and length 18.9 cm. The PSDx (Fig. 4, a, left curve) was not $1/f^\alpha$ in form, partly owing to more rapid fall in log power with increasing log frequency imposed by the impedance of the skull and scalp, and partly due to a spatial spectral peak in the middle spatial frequency range that corresponded to the spatial frequency of the gyri and sulci of the human cerebral hemisphere (Freeman et al. 2003). Derivation of the PSDx in each band of temporally band pass filtered EEG showed that this spatial peak occurred in all temporal frequency bands through beta (Fig. 4, b) and gamma (not reproduced here). This peak in PSDx implied that a temporal EEG impulse was repeatedly synchronized over distances of 10–19 cm covering multiple gyri and sulci.

3.2 Aperiodic phase re-setting of beta-gamma oscillations at alpha-theta rates

This inference gave the hypothesis that the high temporal resolution of instantaneous frequency and phase afforded by HT (Pikovsky et al. 2001) would enable detection of the simultaneous jumps in phase over wide areas of the scalp EEG that would demarcate phase transitions by which neocortex repeatedly re-synchronized beta and gamma oscillations in broad spatial domains. This hypothesis was tested and verified (Fig. 5) in normal human volunteers at rest with eyes

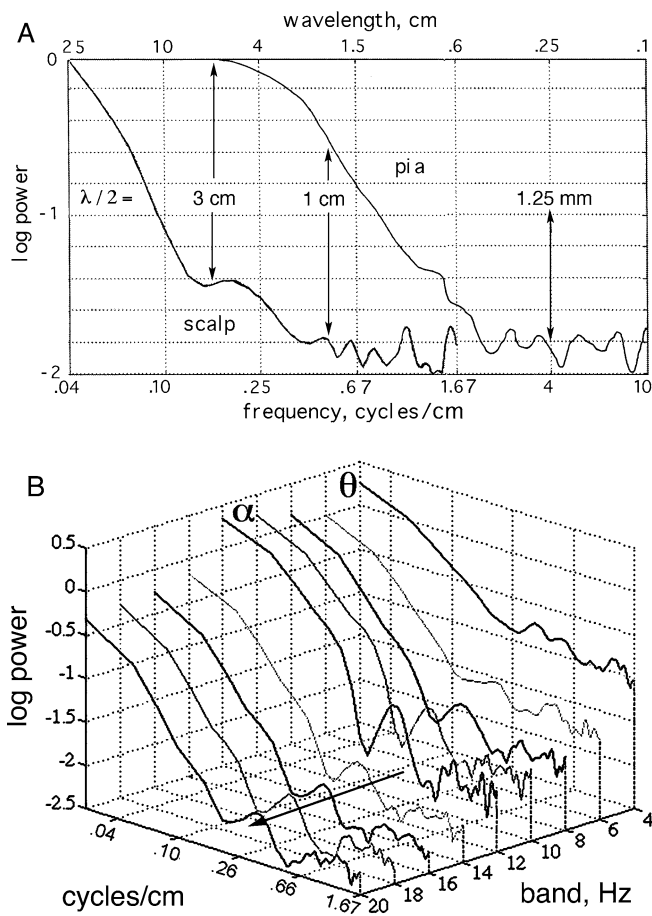


Fig. 4 a pia Spatial power spectral density (PSD_x) from a linear array on a single gyrus in a human subject with spacing of 0.5 mm showing '1/f' scaling. **'Scalp'**: PSD_x from curvilinear scalp array with spacing of 3 mm revealed a peak in the spatial frequency range of gyri and sulci. From Freeman (2000). **b.** The PSD_x of scalp EEG in narrow temporal bands gave the peak in all temporal bands through the gamma range (not included here). That spread was the PSD_t pattern of a temporal impulse that occurred synchronously over 10–19 cm distance on the scalp and repeated nearly periodically in the alpha–theta range. The spatial resolution of gamma activity in scalp EEG extended up to spatial frequencies approaching those of the width of gyri. From Freeman et al. (2003)

closed giving prominent alpha activity, and with eyes open and fixated or engaged in generating weak but controlled electromyographic activity (EMG) by tensing scalp muscles, both of which were intentional actions without bodily movements.

Band-pass filtering enabled application to the broad-spectrum EEG (Freeman et al. 2003). To find the optimum pass band the rate of change in analytic frequency, ω , was calculated from successive phase differences. These revealed plateaus of phase constancy bracketed by simultaneous peaks in coordinated analytic phase differences (CAPD) over long distances (Fig. 5, b).

In some instances they covered the entire array. The jumps in ω recurred at rates in the alpha–theta ranges (Fig. 5, a). The pass band for the HT was optimized by cross-correlating ω

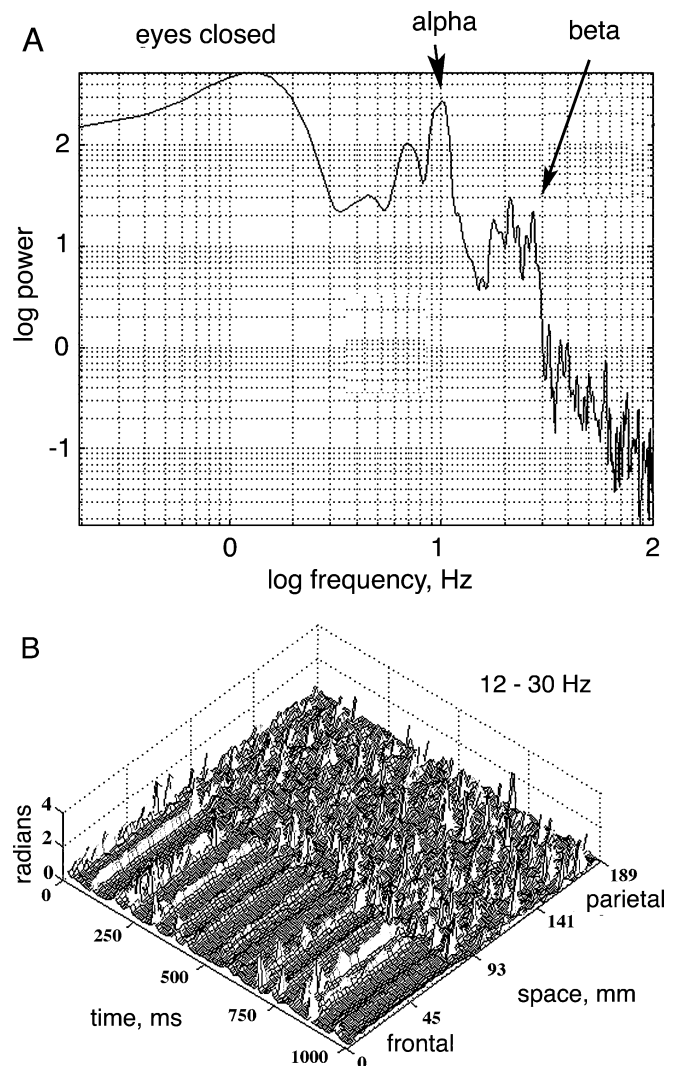


Fig. 5 a The cospectrum of the cross-correlation between the unfiltered EEG and the analytic phase differences on every channel shows peaks in the alpha and beta ranges. **b** The CAPD calculated for the 64 channels after band-pass filtering in the beta range (12–30 Hz) revealed episodic plateaus of phase constancy that were bracketed by jumps in phase that were synchronized over distances varying from a few centimeters to the entire linear array. The spatial standard deviation, $SD_x(t)$, of the CAPD gave a reliable measure of spatial synchrony in scalp EEG. AM patterns are to be sought in plateaus bracketed by phase slip. From Freeman and Rogers (2003)

with the unfiltered EEG repeatedly while varying the cut-off frequencies and measuring the cospectral peak in the alpha range to construct tuning curves for nine subjects; all gave optimal filters in the beta band, 12–30 Hz.

Application of the HT to multiple EEG from an N-array was complicated by the fact that the N-phase values in a stable epoch are distributed in a conic pattern, so that analytic phase from the arctangent gives phase vectors from each electrode that rotate across the imaginary axis at different times. When phase values were unwrapped, the parallel ramps diverged unpredictably in offsets of π or 2π . This problem is solved either by calculating sequential phase differences for

the CAPD (instantaneous frequency, Fig. 5, b), or by restricting measurement of phase cones to time intervals between first and last crossings of the imaginary axis by the vectors (Table 1).

3.3 Comparison of phase from Fourier and Hilbert transforms

Two basic quantities essential to describe spatial patterns of phase: the mean temporal wavelength, W_T , in rad/sec and the mean spatial wavelength, W_X in rad/mm (Freeman 2004a). Table 1 compares summary values of W_T and W_L from the Fourier and Hilbert methods. A statistically significant difference was found only for the phase gradient. This difference was traced to the procedural difference that the Fourier transform (FFT) was restricted to epochs ≥ 32 ms in order to measure frequency in the gamma range from which to calculate the phase, whereas the HT was restricted to epochs ≤ 12 ms in order to avoid the breaks imposed by the calculation of the arctangent (for detailed treatments of the advantages of FFT and HT see Pikovsky et al. 2001; Le Van Quyen et al. 2001; Quiroga et al. 2002).

Table 1 illustrates the types of measurement that are required in order to validate the measures with HT by correlation with those by FFT, and to compare the spatiotemporal properties of phase in humans with those in animals. Data are listed for W_L and W_X from a 1×1 cm 8×8 grid in a human subject. The means and standard deviations (SD) of phase gradients were lower for humans than for animals. However, analysis showed (Freeman 2004b) that the EEG spatial and temporal power spectral densities and the derived measures of cone diameter and duration had power law distributions ($1/f$). Moreover, the means and SDs varied with the duration of temporal windows and the size of electrode arrays; that is, the results of measurement varied with the sizes of the units of measurement. The human grid was 50% larger in area than the rabbit grid, and so were the phase cone diameters, which implied that the underlying distributions were fractal (Mandelbrot 1983; Linkenkaer-Hansen et al. 1999). The further suggestion is that the local dynamics in rabbit and human neocortex are scale-free and therefore basically the same, though human brains are larger, and that the same dynamics may hold in brains of mice and whales across four orders of magnitude in size.

4 Modeling neocortical dynamics with the KV set

4.1 The need for field theory

Unlike the case for KI–KIV sets there is as yet no working mathematical treatment for the KV set. Clearly on the basis of evidence from behavioral (Köhler 1940) and physiological studies the theory must be a field theory. Three such approaches are promising. Neuropercolation (Kozma et al. 2005) is based in random graph theory extended to include

small-world effects and scale-free networks (Wang and Chen 2003). Another route may be to exploit electric and magnetic field theory (Barrett 1993, 2000, 2001). A third may be to explore quantum field theory as distinct from quantum mechanics (Pessa 2000; Vitiello 2001; Potapov and Ali 2001). The latter two avenues are mere suggestions; only neuropercolation has been developed past the stage of speculation.

The need for field theories is illustrated in Fig. 2, which reveals a fundamental difference between the three-layered paleocortex (as embodied in the olfactory bulb) and six-layered neocortex. In the OB only one phase cone at a time covers the bulb with each inhalation, as shown by a single apex with multiple phase gradients for different frequencies but invariant phase velocity. In neocortices multiple phase cones overlap at all times, each with its own apex and gradient. Under the interpretation that phase cones reveal local phase transitions, they resemble bubbles in a pan of boiling water. This difference between three-layered paleocortex and six-layered neocortex has great theoretical significance, because it indicates that, unlike the OB, the neocortex undergoes multiple small phase transitions, most of which are rapidly quenched, and some of which grow into large-scale changes that are identified with new AM patterns. Prigogine (1980) described chemical reaction systems as maintaining self-stabilized structures that he called “dissipative systems,” because they formed far from equilibrium and fed on energy.

The process by which neocortex maintains its stability while forming AM patterns by repeated phase transitions resembles a state of self-organized criticality (Bak 1996; Jensen 1998). The classic model for SOC is the sand pile that maintains its critical slope by repeated avalanches having random locations and times of onset, overlap and fractal distributions of size and duration. These properties are very similar to those of neocortical phase cones. Although there is no widely accepted theory to support SOC, the metaphor points a potentially fruitful way to analyze the field dynamics of neocortex. The implication is that neocortex maintains a stable state through local feedback control of neural firing rates everywhere in neocortex (Freeman 1975, 2000) by homeostatically regulating the gain of synaptic interaction. Under impact of input to each local area of cortex, the area tends to be destabilized owing to the input-dependent gain of all KI sets, so that the oscillations in the “spontaneous” background EEG reflect the work done by neocortex to regain its basal state. The mean level of firing rates is comparable to the critical angle of the sand pile, and to the transition temperature of a pan of boiling water. The generalized feedback gain constitutes an order parameter (Haken 1983). In this context the peaks in the power spectrum show oscillations that are equivalent to avalanches by which neocortex maintains its stability under perturbation by sensory and other control parameters, mainly thalamic (Miller and Schreiner 2000). The fractal distributions imply that the state of SOC is scale-free (Wang and Chen 2003). CAPD are invariably found in EEG from intracranial grids fixed in rabbits and the human subject. There are no normative sizes, durations or numbers of neocortical phase cones or CAPD; the CAPD jumps in scalp EEG may

Table 1 Mean \pm SD of phase parameters: FFT/Hilbert

Subject	N/s	Frequency (Hz)	Gradient (rad/mm)	W_T (ms/rad)	W_X (mm/rad)
<i>N</i> = 6 rabbits					
Mean FFT	10.2	32.7 \pm 4.8	0.111 \pm 0.040 ^b	5.36 \pm 1.38	11.4 \pm 4.1
Mean HT	32.4	38.8 \pm 4.3	0.158 \pm 0.048 ^b	4.41 \pm 0.46	7.7 \pm 2.7
<i>N</i> = 1 subject					
Human FFT ^a	5.1	26.5 \pm 1.9	0.066 \pm 0.017 ^c	6.0 \pm 0.4	15.5 \pm 4.7
Human HT ^a	21.7	31.5 \pm 3.8	0.092 \pm 0.030 ^c	5.13 \pm 0.70	11.7 \pm 3.9

^aFrom Freeman (2004b), 25–50 Hz, window 200 ms, <30% residuals

^b*p* < 0.01

^c*p* < 0.001

The two basic parameters of neocortical EEG, temporal wavelength, W_T , and spatial wavelength, W_X , were evaluated by the FFT and HT methods. The steeper gradient by HT was due to its short window. Convergence of the spatial parameters by FFT/HT proved success in solving the HT problem of multiple channels. From Freeman (2004b)

constitute the tails of fractal distributions, which represent neocortical phase transitions that extend widely over each hemisphere and may include multiple sensory areas.

Documenting the spatiotemporal phase infrastructure of neocortical EEG is critical for guiding the design of small-world, scale-free networks to model the dynamics by which neocortex combines flexibility with stability and integrates multisensory information with memory into Gestalts. For example, a key finding to be explained is the random variation in phase cones between maximal lead (“explosion”) and maximal lag (“implosion”) at the apex (Fig. 2, b), which might be modeled as a saddle node or subcritical Hopf bifurcation in a distributed network (Freeman and Barrie 2000; Freeman 2003b, 2004b).

4.2 Sensorimotor integration

The emphasis in this report is placed on the input phase of the action-perception cycle and on the global form of the closure of the cycle from perception leading to renewed action. Houk (2005) describes the output stages of the cycle. Indisputably description and analysis of the structure and function of both phases of the cycle are best undertaken by recognizing and taking advantage of the modules on which both phases depend. The modularization on the sensory side is more obvious, first in terms of sensory modality and then within each modality the multiple partitions in both series and in parallel within each sensory cortical domain. Houk demonstrates the comparable modularization on the motor side in terms of the parallel feedback loops that engage cortex with the basal ganglia, midbrain, pons and cerebellum.

Analysis in terms of modularization has led to an intractable problem in both phases of the action-perception cycle. On the input side there is the unresolved issue of the binding problem (Singer and Gray 1995); how are the features of objects combined to form object representations, and how are representations contextualized into the whole history of the individual subjects? On the output side there is the unresolved issue of the intent of “voluntary” action; how is the entire forebrain mobilized into the organization of an action that is directed toward the achievement of a centrally spec-

ified goal? Houk raises the problem by focusing on areas 46 and M1, in which for each DPM he postulates multiple inputs containing perceptual information and a scalar input of a neuromodulator containing an evaluation, such as dopamine mediating reward, leading to a vector output by the basal ganglia to cortex and brainstem that directs a skilled action. This he proposes “modulates pattern classification on two time scales,” immediate decision and long-term incremental consolidation of synaptic strengths. However, his modular net does not specify the number and type of classes of skilled actions or their scales in time and space, leading to the combinatorial problem that a module might be required for each skilled action as, for example, one DPM for each sport, and further, one each for backstroke and breaststroke in swimming, for forehand or backhand in tennis, for pitching and batting in baseball and so on. His suggestion that “global neuromodulatory mechanisms” may contribute more importantly to “the shaping of collective behavior” does not account for brain capacity for sudden large-scale reorganizations of the modules in adaptive behaviors, because the time scales for neuromodulators in his model are too slow.

4.3 Conclusions and summary

The intent of this report is to propose a resolution of the intractable problems in both neural networks and in brain imaging by addressing the manner in which both local and global cortical patterns of synchronized activity can be observed and measured using the EEG. The critical inference to be drawn from the multichannel EEG data is that phase transitions occur over large fractions of each cerebral hemisphere, by which the oscillations of populations of neurons in the beta and gamma ranges are repeatedly re-initialized, re-synchronized within very few milliseconds (Freeman 2005), and then re-stabilized with a new AM pattern for three to five cycles of the center frequency of the shared carrier wave, while the intensity of pattern transmission rises to a maximum (Freeman 2004a, 2005). The high-intensity broadcasts of synchronized carrier waves bearing stable AM pattern are predicted to have major impact on those brain stem structures that receive and are tuned to input from cortical components

of DPMs (Houk 2005), which by their vector outputs initiate and maintain the corrections and refinements that are necessary for both skilled action and thinking.

The hypothesis proposed here for future testing is that the EEG contains both global and local AM patterns. These patterns may be used to locate active modules, and to determine their orderly sequences during the performance of simple voluntary actions triggered by sensory cues. Just as filters are used to separate action potentials from dendritic potentials in extracellular recording from microelectrodes, low-pass and high-pass filters can be applied jointly to EEG to extract both the local mesoscopic signals and the encompassing global macroscopic signals for the synthesis of models that capture sensorimotor integration implementing the action-perception cycle. Details on the techniques needed to pursue this program are described in the Appendices of a three-part series in *Clinical Neurophysiology* (Freeman 2004a,b, 2005).

Acknowledgements This study was supported by grant MH 06686 from the National Institute of Mental Health, grant NCC 2-1244 from the National Aeronautics and Space Administration and grant EIA-0130352 from the National Science Foundation to Robert Kozma.

References

- Bak P (1996) *How nature works: self-organized criticality*. Copernicus, New York
- Barrett TW (1993) Electromagnetic phenomena not explained by Maxwell's equations. In: Lakhtakia A (ed) *Essays on the formal aspects of electromagnetic theory*. World Scientific Publishing, Singapore
- Barrett TW (2000) Topology and the physical properties of the electromagnetic field. *Apeiron* 7:3–11
- Barrett TW (2001) Topological approaches to electromagnetism. In: Evans M (ed) *Modern nonlinear optics*, 2nd edn. Wiley Interscience, New York, pp 699–734
- Barrie JM, Freeman WJ, Lenhart M (1996) Modulation by discriminative training of spatial patterns of gamma EEG amplitude and phase in neocortex of rabbits. *J Neurophysiol* 76:520–539
- Braitenberg V, Schüz A (1991) *Anatomy of the cortex: statistics and geometry*. Springer, Berlin Heidelberg New York
- Freeman WJ (1975) *Mass action in the nervous system*. Academic, New York. Available in electronic form on <http://sulcus.berkeley.edu>
- Freeman WJ (1987) Simulation of chaotic EEG patterns with a dynamic model of the olfactory system. *Biol Cybern* 56:139–150
- Freeman WJ (2000) *Neurodynamics: an exploration of mesoscopic brain dynamics*. Springer-Verlag, London
- Freeman WJ (2003a) A neurobiological theory of meaning in perception. Part 1. Information and meaning in nonconvergent and nonlocal brain dynamics. *Int J Bifurc Chaos* 13:2493–2511
- Freeman WJ (2003b) A neurobiological theory of meaning in perception. Part 2. Spatial patterns of phase in gamma EEG from primary sensory cortices reveal the properties of mesoscopic wave packets. *Int J Bifurc Chaos* 13:2513–2535
- Freeman WJ (2003c) The wave packet: an action potential for the 21st century. *J Integrat Neurosci* 2:3–30
- Freeman WJ (2004a) Origin, structure, and role of background EEG activity. Part 1. Analytic phase. *Clin Neurophysiol* 115:2077–2088
- Freeman WJ (2004b) Origin, structure, and role of background EEG activity. Part 2. Analytic amplitude. *Clin Neurophysiol* 115:2089–2107
- Freeman WJ (2005) Origin, structure, and role of background EEG activity. Part 3. Neural frame classification. *Clin Neurophysiol* (in press).
- Freeman WJ, Baird B (1987) Relation of olfactory EEG to behavior: spatial analysis. *Behav Neurosci* 101:393–408
- Freeman WJ, Barrie JM (2000) Analysis of spatial patterns of phase in neocortical gamma EEGs in rabbit. *J Neurophysiol* 84:1266–1278
- Freeman WJ, Burke BC (2003) A neurobiological theory of meaning in perception. Part 4. Multicortical patterns of amplitude modulation in gamma EEG. *Int J Bifurc Chaos* 13:2857–2866
- Freeman WJ, Burke C, Holmes MD (2003) Aperiodic phase re-setting in scalp EEG of beta-gamma oscillations by state transitions at alpha-theta rates. *Hum Brain Mapp* 19:248–272
- Freeman WJ, Burke BC, Holmes MD, Vanhatalo S (2003) Spatial spectra of scalp EEG and EMG from awake humans. *Clin Neurophysiol* 114:1055–1060
- Freeman WJ, Chang H-J, Burke BC, Rose PA, Badler J (1997) Taming chaos: stabilization of aperiodic attractors by noise. *IEEE Trans Circuits Syst* 44:989–996
- Freeman WJ, Gaál G, Jornten R (2003) A neurobiological theory of meaning in perception. Part 3. Multiple cortical areas synchronize without loss of local autonomy. *Int J Bifurc Chaos* 13:2845–2856
- Freeman WJ, Grajski KA (1987) Relation of olfactory EEG to behavior: factor analysis. *Behav Neurosci* 101:766–777
- Freeman WJ, Rogers LJ (2002) Fine temporal resolution of analytic phase reveals episodic synchronization by state transitions in gamma EEG. *J Neurophysiol* 87:937–945
- Freeman WJ, Rogers LJ (2003) A neurobiological theory of meaning in perception. Part 5. Multicortical patterns of phase modulation in gamma EEG. *Int J Bifurc Chaos* 13:2867–2887
- Freeman WJ, Rogers LJ, Holmes MD, Silbergeld DL (2000) Spatial spectral analysis of human electrocorticograms including the alpha and gamma bands. *J Neurosci Meth* 95:111–121
- Freeman WJ, Schneider W (1982) Changes in spatial patterns of rabbit olfactory EEG with conditioning to odors. *Psychophysiol* 19:44–56
- Freeman WJ, Viana Di Prisco G (1986) Relation of olfactory EEG to behavior: time series analysis. *Behav Neurosci* 100:753–763
- Friston KJ (2000) The labile brain. I. Neuronal transients and nonlinear coupling. *Phil Trans R Soc Lond B* 355:215–236
- Gibson JJ (1979) *The ecological approach to visual perception*. Houghton Mifflin, Boston
- Haken H (1983) *Synergetics: an introduction*. Springer, Berlin Heidelberg New York
- Herrick CJ (1948) *The brain of the tiger salamander*. University of Chicago Press, Chicago
- Houk J (2005) Agents of the mind. *Biol Cybern* (this issue)
- Jensen HJ (1998) *Self-organized criticality: emergent complex behavior in physical and biological systems*. Cambridge UP, New York
- Köhler W (1940) *Dynamics in psychology*. Grove Press, New York
- Kozma R, Freeman WJ (2001) Chaotic resonance: methods and applications for robust classification of noisy and variable patterns. *Int J Bifurc Chaos* 10:2307–2322
- Kozma R, Freeman WJ (2002) Classification of EEG patterns using nonlinear dynamics and identifying chaotic phase transitions. *Neurocomputing* 44:1107–1112
- Kozma R, Freeman WJ (2003) Basic principles of the KIV model and its application to the navigation problem. *J Integr Neurosci* 2:125–145
- Kozma R, Freeman WJ, Erdí P (2003) The KIV model – nonlinear spatio-temporal dynamics of the primordial vertebrate forebrain. *Neurocomput* 52:819–826
- Kozma R, Puljic M, Balister P, Bollabás B, Freeman WJ (2005) Phase transitions in the neuropercolation model of neural populations with mixed local and non-local interactions. *Biol Cybern* (this issue)
- Le Van Quyen M, Foucher J, Lachaux J-P, Rodriguez E, Lutz A, Martinerie J, Varela F (2001) Comparison of Hilbert transform and wavelet methods for the analysis of neuronal synchrony. *J Neurosci Meth* 111:83–98
- Linkenkaer-Hansen K, Nikouline VM, Palva JM, Ilmoniemi RJ (2001) Long-range temporal correlations and scaling behavior in human brain oscillations. *J Neurosci* 15:1370–1377
- Mandelbrot BB (1983) *The fractal geometry of nature*. Freeman, San Francisco

- Miller LM, Schreiner CE (2000) Stimulus-based state control in the thalamocortical system. *J Neurosci* 20:7011–7016
- Ohl FW, Scheich H, Freeman WJ (2001) Change in pattern of ongoing cortical activity with auditory category learning. *Nature* 412:733–736
- Ohl FW, Deliano M, Scheich H, Freeman WJ (2003) Early and late patterns of stimulus-related activity in auditory cortex of trained animals. *Biol Cybern*, p 6. online: DOI 10.1007/s00422-002-0389-z
- Pessa E (2000) Cognitive modeling and dynamical systems theory. *La Nuova Critica* 1(35):53–94
- Potapov AB, Ali MK (2001) Nonlinear dynamics and chaos in information processing neural networks. *Diff Eq Dyn Syst* 9:259–319
- Prigogine I (1980) *From being to becoming: time and complexity in the physical sciences*. Freeman, San Francisco
- Principe JC, Tavares VG, Harris JG, Freeman WJ (2001) Design and implementation of a biologically realistic olfactory cortex in analog VLSI. *Proc IEEE* 89:1030–1051
- Pikovsky A, Rosenblum M, Kurths J (2001) *Synchronization – a universal concept in non-linear sciences*. Cambridge UP, UK
- Quiroga RQ, Kraskov A, Kreuz T, Grassberger P (2002) Performance of different synchronization measures in real data: A case study on electroencephalographic signals. *Physical Rev E*, 6504:U645-U6 58-art. no. 041903
- Rodriguez E, George N, Lachaux J-P, Martinerie J, Renault B, Varela F (1999) Perception’s shadow: long-distance synchronization of human brain activity. *Nature* 397:430–433
- Sholl DA (1956) *The organization of the cerebral cortex*. New York: Wiley
- Singer W, Gray CM (1995) Visual feature integration and the temporal correlation hypothesis. *Ann Rev Neurosci* 18:555–586
- Stam CJ, Breakspear M, van Cappellen van Walsum A-M, van Dijk BW (2003) Nonlinear synchronization in EEG and whole-head recordings of healthy subjects. *Hum Brain Mapp* 19:63–78
- Tallon-Baudry C, Bertrand O (1999) Oscillatory gamma activity in humans and its role in object representation. *Trends Cogn Sci* 3:151–162
- Tass P, Rosenblum MG, Weule J, Kurths J, Pikovsky AS, Volkman J, Schnitzler A, Freund H-J (1998) Detection of n:m phase locking from noisy data: Application to magnetoencephalography. *Physical Rev Lett* 81:3291–3294
- Tolman EC (1948) Cognitive maps in rats and men. *Psychol Rev* 55:189–208
- Tsuda I (2001) Toward an interpretation of dynamics neural activity in terms of chaotic dynamical systems. *Behav Brain Sci* 24:793–847
- Varela F, Lachaux J-P, Rodriguez E, Martinerie J (2001) The brain-web: phase synchronization and large-scale integration. *Nat Rev Neuro* 2:229–239
- Vitiello G (2001) *My double unveiled. The dissipative quantum model of brain*. Benjamin, Amsterdam
- Wang XF, Chen GR (2003) Complex networks: small-world, scale-free and beyond. *IEEE Circuits Syst* 31:6–2
- Watts DJ, Strogatz SH (1998) Collective dynamics of ‘small-world’ networks. *Nature* 393:440–442

Query

1. Linkenkaer–Hansen et al. 1999 is cited in the text but not in the reference list.
2. Please check the page range for the reference Wang and Chen (2003)